Hydrodynamics of a Tropical Coastal Lagoon Influenced by Monsoon and Outer Sea Conditions: A Case Study of Ao Kung Krabaen Lagoon-Thailand

Tanuspong Pokavanich* and Kittipong Phattananuruch

ABSTRACT

Ao Kung Krabaen Lagoon (AKBL) is a small and shallow coastal lagoon situated in the eastern part of Thailand. It is an important "Blue Carbon" ecosystem of this region. However, water quality of the lagoon has drastically deteriorated in recent years. To counteract the problem, a comprehensive understanding of water circulation within the lagoon and exchange with the outer sea is needed. In this study, seasonal field observations were made and then applied in three-dimensional hydrodynamic simulations using Delft3D-FLOW. Results indicate that water properties, water circulation and water exchange differ notably by season. During the southwest (SW) monsoon (July-September), circulation is at its strongest, and there are strong double-gyre circulations. This results in enhancing exchange with the sea, hence significantly reducing flushing time. The flushing time during the SW monsoon is approximately three days. During the transition period (April-May) between the northeast monsoon and the SW monsoon, sluggish circulation dominates the lagoon. The flushing time increases to around 10 days, which is the annual maximum. Water circulation within the lagoon is mostly in two-dimensional patterns owing to its shallowness, even though water exchange occurs in three dimensions. This study also demonstrates that the tropical coastal lagoons scattered around the world should be considered three-dimensionally and with attention to varying water density both inside and outside the lagoon to properly model their hydrodynamics and exchange with the outer sea.

Keywords: Exchange rate, Density-driven current, Direct-precipitation, Flushing rate, Monsoonal wind, Three-dimensional simulation

INTRODUCTION

Coastal lagoons are among the most common coastal environments, occupying about 13 % of the world's coastlines (Barnes, 1980). In Asia, coastal lagoons occupy about 13.8 % of the coastline. They can be generally classified as choked lagoons, restricted lagoons or leaky lagoons depending on their interaction with the outer sea. The choked lagoons have the least interaction (the least water exchange between the lagoon and the outer sea). The leaky lagoons have the strongest interaction, while the restricted lagoons are intermediate between the other two (Kjerfve, 1986). The coastal lagoons are also important as coastal ecosystems. They represent the boundary (or ecotone) between terrestrial and marine habitats. Ecotones are high in biodiversity and ecosystem services (Sriyanie, 2013).

Ao Kung Krabaen Lagoon (AKBL) is an important ecotone situated in the eastern part of Thailand, approximately 240 km from Bangkok. The lagoon was once part of the sea but became separated by sediment from eroding mountains and rivers during the Holocene's sea level rise (Kung

Department of Marine Science, Faculty of Fisheries, Kasetsart University, Bangkok, Thailand
* Corresponding author. E-mail address: ffistop@ku.ac.th
Received 9 July 2021 / Accepted 11 February 2022

Krabaen Bay Royal Development Study Center, pers. comm.). The lagoon is shallow, with average depth of around 0.8 m. Water depth at the mouth is around 5 m. It has a wet area of approximately 6.7 km^2 and a wet perimeter of approximately 10.5 km during high tide. These values significantly decrease during low tide. The lagoon has a maximum length of 3.5 km, oriented northwest to southeast, and a width of 2.3 km (Figure 1). It has one connection (mouth) to the outer sea that is approximately 380 m wide.

The AKBL supports tourism, local fisheries and aquaculture, and it hosts one of the most fertile seagrass beds and mangrove forests in the area. Recently, the lagoon has received more attention and study because of its increasing importance as a "Blue Carbon" ecosystem in the region. The lagoon is surrounded by mangrove forests and intensive shrimp farms. Previous studies have reported that the farms are sources of high-nutrient wastewater that cause deterioration of water quality within the lagoon (e.g., Sangrungruang *et al*., 1999; Satumanatpan *et al*., 2011). At present, the shrimp farms are unable to use raw water from the lagoon directly due to its poor quality. Instead, the farms depend on expensive seawater irrigation systems that take raw water directly from the outer sea. In the near future, the water quality problems could become more severe and further impair the lagoon's ecosystem and services. Hence, more than ever, effective management of the lagoon system is needed. This can be done only with comprehensive understanding of the lagoon's system of water movements (Guyondet and Koutitonsky, 2008).

One of the first hydrodynamic studies of AKBL was by Sasaki and Inoue (1985). They described the fluctuating water level and tidal currents within the lagoon using simple field observations. Pokavanich et *al*. (2018) applied a two-dimensional hydrodynamic model to investigate tide-driven and wind-driven currents within the

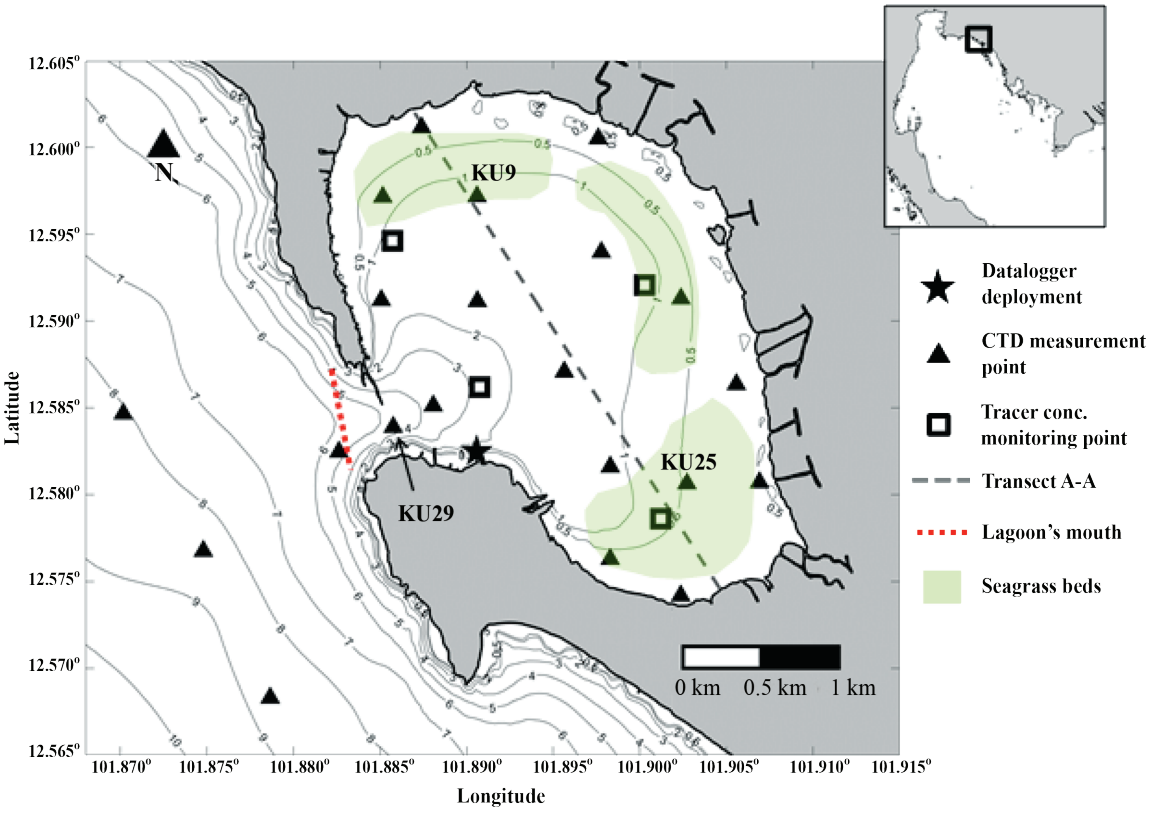

Figure 1. Location of AKBL (inset), and field observation and monitoring points.

lagoon. They successfully calibrated their model with limited field data and reported detailed patterns of seasonal currents. They also showed that the tidal ranges of the lagoon were between 0.6 and 1.6 m, corresponding to current speeds of 0.15 and 0.42 $m \cdot s^{-1}$ during neap and spring tides, respectively. Based on numerical experiments, they also presented evidence showing significant potential variation in both water circulation and exchange over the course of a year.

Despite the importance of AKBL and its water quality problems, the lagoon's three-dimensional hydrodynamic system (including effects of water density) has not been adequately investigated and is poorly understood. However, there is evidence indicating significant annual variations of salinity and water temperature (both affecting water density) of the lagoon. These variations could affect the behavior of water in the lagoon, since the interplay of topography, wind stress, tidal current and water density has been reported to determine water circulation and exchange in other coastal lagoons in the world (e.g., Kjerfve,1986; Sylaios *et al*., 2005; Guyondet and Koutitonsky, 2008; Kennish and Paerl, 2010; Umgiesse *et al*., 2014).

This study presents fully three-dimensional hydrodynamic features of AKBL based on data obtained from comprehensive field measurements and three-dimensional hydrodynamic and conservative tracer simulations. We illustrate and discuss controlling mechanisms of fundamental seasonal oceanographic characteristics within the lagoon, circulation within the lagoon, and exchange between the lagoon and the outer sea. Findings from this study can contribute to the understanding of other small coastal lagoons distributed widely in tropical areas.

MATERIALS AND METHODS

Field observations

Three intensive field observation campaigns were carried out during the southwest monsoon (SW monsoon) in July-August 2018, during the northeast monsoon (NE monsoon) in December 2018 and during the transition from the NE monsoon to the SW monsoon (Transition 1) in April 2019. No observations were made during the transition from SW monsoon to NE monsoon (Transition 2) in October 2018. Measurements of horizontal and vertical distributions of water temperature and salinity inside the lagoon were made with CTD sensor (YSI 556 multi-parameter probe, U.S.A.). Flow velocity profiles were measured across the lagoon mouth using an acoustic Doppler current profiler (ADCP) sensor (Teledyne RDI Instrument, U.S.A.) deployed face-down with bottom tracking functionality. HOBO-WLL and HOBO-Conductivity data loggers (Onset Inc., U.S.A.) were deployed nearthe lagoon's mouth (Figure 1) to measure water level, water temperature and salinity at 30 min intervals.

Numerical modeling

Hydrodynamic and conservative tracer simulations were carried out in this study using Delft3D-FLOW (Deltares, 2018a) and Delft3D-WAQ (Deltares, 2018b) programs, respectively. The hydrodynamic model is fully three-dimensional, taking into account combined effects of tide, wind and water density (governed by water temperature and salinity). The Delft3D-FLOW has two domains, encompassing the whole Gulf of Thailand (GOT) and herein called "GOT model", and the coastal sea of Chanthaburi Province with AKBL at the center (AKBL model) (Figure 2).

The models were calibrated and validated against field-measured data. Sea bottom roughness was set to uniformly distributed using a Chezy coefficient of 65 $m^{1/2} \cdot s^{-1}$. Background vertical eddy viscosity and diffusivity were 0.0006 $m^2 \cdot s^{-1}$. Other general model setup parameters are shown in Table 1. River discharge data were acquired from the Global Flood Awareness System (Harrigan *et al*., 2019), and show that Prasae River's discharge peaks around September-October with values of around 40-60 $m^3 \cdot s^{-1}$. The discharge decreases to less than 10 $m^3 \cdot s^{-1}$ for the rest of the year. Meteorological forcing was derived from the ECMWF-ERA5 dataset (Hersbach *et al*., 2018a; 2018b). The total precipitation data from the ERA5 was increased by 1.8 times to better match the observed values from the Thailand

Table 1. General hydrodynamic model setup.

	GOT model	**AKBL model**
Simulation period/Time step	1 January 2018 to 1 January 2021/3 min	
Grid/vertical layer	Rectangular with 10 sigma coordinate layers (2, 6, 8, 10, 10, 10, 10, 12, 14, 18)	Curvilinear with 10 sigma coordinate layers as in the the GOT model
Initial conditions/Spin up	Uniformly rested water with temperature 28 ºC, salinity 31 psu/2 years	Uniformly rested water with temperature 30 ºC, salinity 32 psu/6 months
Heat flux model	Ocean model (Deltares, 2018a)/Secchi depth = 5 m/Dalton and Stanton no. = 0.0013	
Meteorological forcing	ERA5 hourly data from 1979 to present (Hersbach *et al*., 2018a; 2018b)	
Wind drag coefficient	Two breakpoints (Deltares, 2018a) 0.00063 and 0.004 at 0 and 25 $m \cdot s^{-1}$	
Offshore boundary	Global Ocean Physics Reanalysis (Global Monitoring and Forecasting Center, 2018) and Global Ocean 1/12o Physical Analysis and Forecast Updated Daily (Global Monitoring and Forecasting Center, 2016)	From GOT model
River	River discharge from the Global Flood Awareness System (Harrigan *et al*., 2019)	Modified Global Flood Awareness System
Background horiz. eddy viscosity/diffusivity.	10/30 $m^2 \cdot s^{-1}$	5/10 $m^2 \cdot s^{-1}$

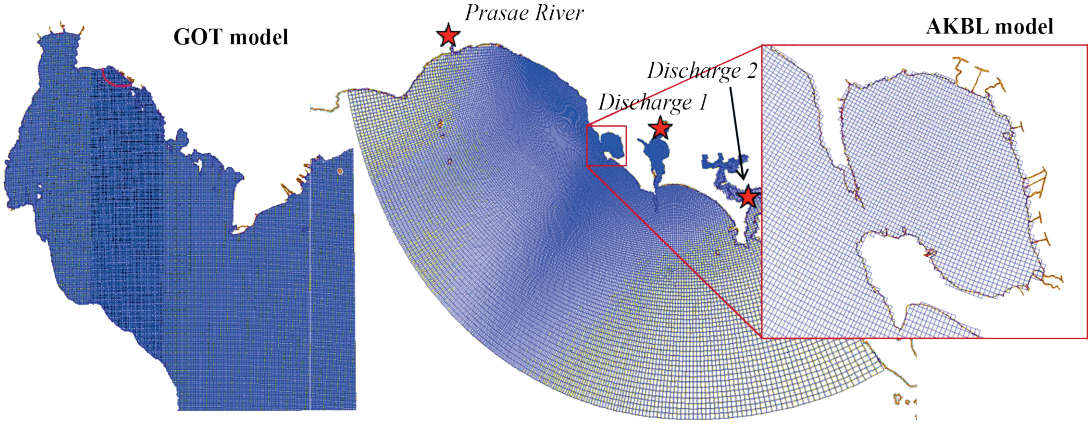

Figure 2. Grids for simulations of the GOT model and the AKBL model.

Meteorological Department's Chanthaburi Province Station (not shown here). This is to account for arbitrary unreliable data of the ERA5 (Hersbach *et al*., 2020). To take into consideration additional freshwater influxes (i.e., from direct runoff along the coasts and submarine groundwater discharge in this region) needed to provide realistic seasonal variation of seawater salinity in this area, discharge rates at Prasae River were doubled and two additional freshwater discharge points (see Figure 2) were added to the model with half of Prasae River's rates.

Delft3D-WAQ simulations were only run for the AKBL model using flow and mixing conditions from the hydrodynamic model. A constant 100 $kg \cdot m^{-3}$ concentration of a conservative tracer was uniformly released at every layer within the lagoon. The concentration of the tracer elsewhere was set to zero. The releases were made at peak spring tides of every simulation period. Changes in tracer concentration within the lagoon were monitored at four points (locations indicated in Figure 1). Concentrations at each point were averaged over 24-h periods for use in the analysis. Hydrodynamic characters and water residence times were analyzed using values averaged over each monsoonal period: SW monsoon-July and August 2018; Transition 2-October 2018; NE monsoon-December 2018 and January 2019; Transition 1-April and May 2019.

RESULTS AND DISCUSSION

Field observed data

Examples of the water temperature and salinity values measured at the inner of part of the lagoon (Station KU9 and Station KU25) and at the mouth (Station KU29) are shown in Figure 3. The results correspond well with our hypotheses regarding notable seasonal variations of water temperature and salinity in the lagoon. During Transition 1, water temperature and salinity were at their highest levels. Water temperature was lowest during the NE monsoon, while salinity was lowest during the SW monsoon. Salinity differences between monitoring stations were the most pronounced during the SW monsoon, when the salinity at the mouth was higher than at stations within the lagoon. There was no significant vertical variation in the measured water temperature or salinity.

Flow data measured by ADCP at the lagoon mouth shows how flow velocity and direction vary by depth. The flow velocity data shown in Figure 4 were collected during the ebb and flood tides at the spring tide of the SW monsoon. During ebb tide, measurements show a strong tidal current with speed of about 0.35 $m \cdot s^{-1}$ flowing out of the lagoon. Weaker currents flowing in the opposite direction were measured at the northern bank of the mouth and along

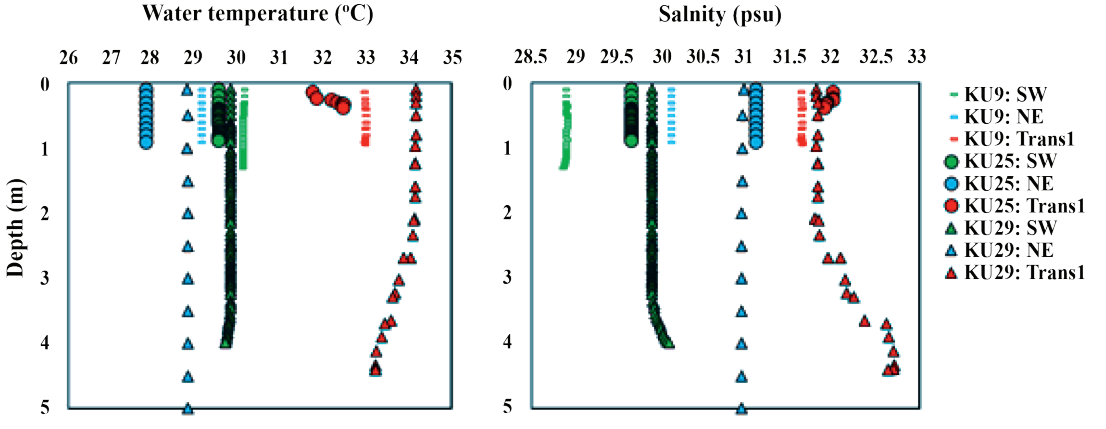

Figure 3. Water temperature and salinity profiles measured at different monsoonal periods (SW, NE, and transition from NE to SW) at the lagoon's mouth (KU29), and at northern (KU9) and southern parts (KU25) of the lagoon.

the deeper layers. The current at the northern bank is part of an eddy formed at the lee side of the lagoon's mouth. However, the current along the deeper layers might be associated with the thermohaline (density-driven) current induced by water density differences between the lagoon and the outer sea. During the flood tide the lower layers of water flow with greater speed because the tidal-driven current and density-driven current flow in the same direction.

Model validation

The GOT model was first validated against water level measurements from secondary sources at three locations around the GOT. The simulated and measured values showed good agreement (data not shown). The AKBL model was then spatially and temporally validated with the observations. Figure 5 shows model validation against measured data near the lagoon's mouth, suggesting that the AKBL model can reproduce realistic diurnal and seasonal oceanographic characters well. The root-mean-square error (RMSE) between the measured and simulated water level, water temperature, and salinity ranges were 0.14-0.16 m, 0.65-1.11 °C, and 0.35-0.55 psu, while the R-Square values ranged from 0.89-0.90, 0.37-0.67, and 0.10-0.41, respectively. The model could also reproduce daily variations of measured salinity, which appeared more significant during the SW monsoon than in the NE monsoon or Transition 1. Results from field data (Figure 3) and simulated data (shown later in this paper) similarly show that during the SW monsoon, salinity inside the lagoon is lower than the outer sea locations, even though the outer sea is closer to sources of freshwater, i.e., Prasae River and other discharge points. This illustrates the importance of direct precipitation as a source of freshwater to dilute seawater within the lagoon during the SW monsoon, which was successfully simulated by our model.

Water level variation

Simulated water level of AKBL is shown in Figure 6. It can be seen that water level variation within the lagoon is significantly influenced by water level of the outer sea. Water level of AKBL is controlled by the diurnal tide of the GOT. Tidal ranges vary by approximately 1.8 m and 0.6 m during spring and neap tides, respectively. Mean water level increases during the NE monsoon and decreases during the SW monsoon over a 40-50 cm range, and is affected by monsoonal Ekman transport (Higuchi *et al*., 2020).

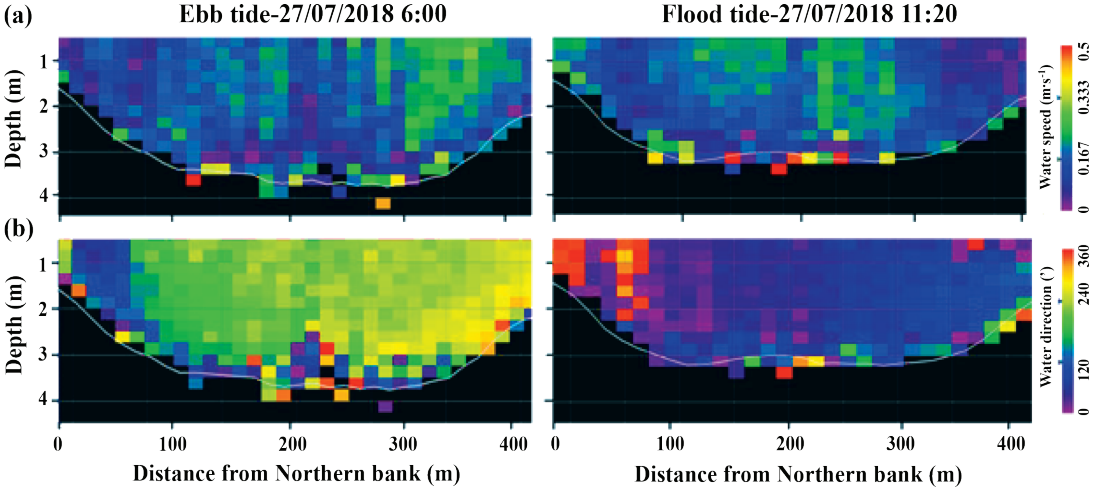

Figure 4. Measurements from acoustic Doppler current profiler across the lagoon mouth during the SW monsoon showing (a) flow speed and (b) flow direction during ebb and flood tides.

During low tides, large areas of the lagoon become dry because of the lagoon's shallowness. Because of the mean water level variation, the extent of this dry area varies seasonally. At low tides around June, the dry area reaches its greatest extent, equaling approximately 60 % of the maximum wet area of the lagoon. During this time, low tides occur in the daytime (see Figure 6). The low tides shift to nighttime from September to March. These seasonal changes in water level and

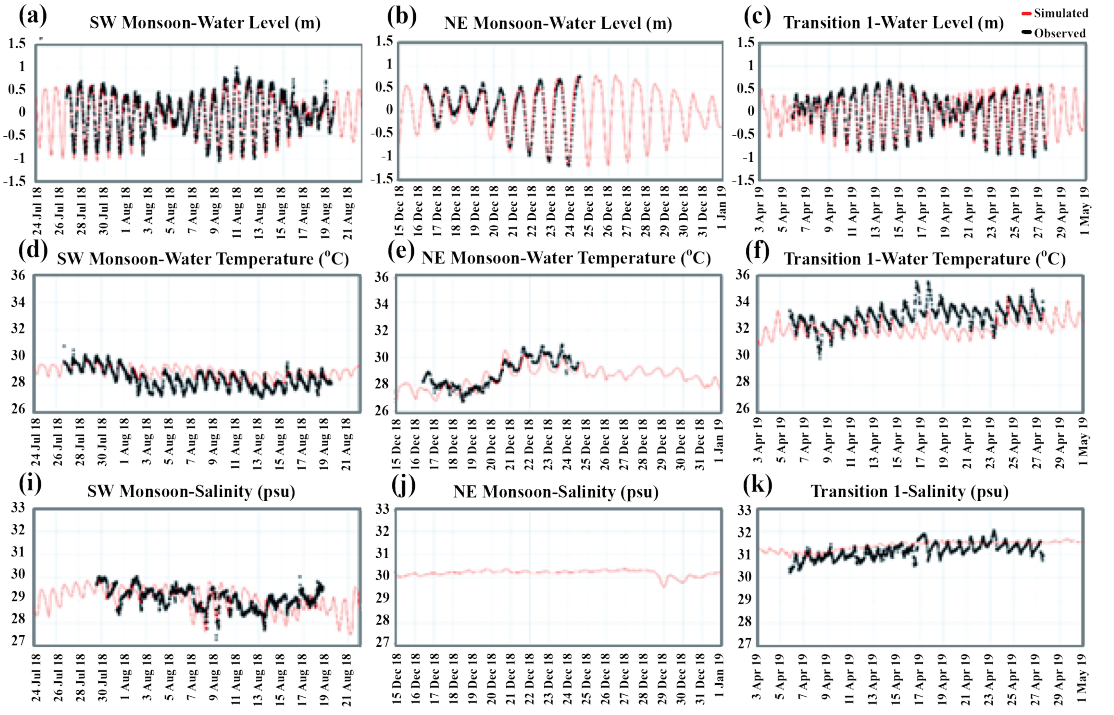

Figure 5. Time-series comparisons of water level (a, b, c), water temperature (d, e, f) and salinity (i, j, k) between simulated and measured values for AKBL during different monsoon periods (SW, NE, and transition from NE to SW).

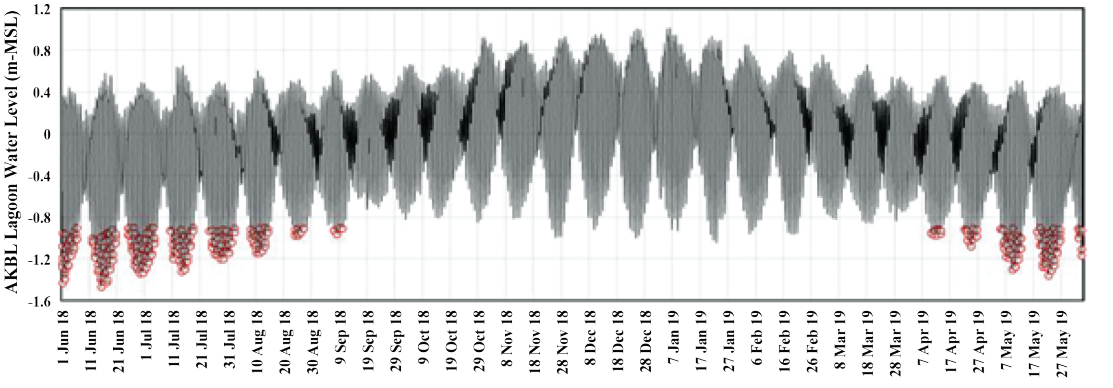

Figure 6. Simulated water level variation of AKBL, with red circles indicating low tides occurring during daytime.

exposure of the lagoon bottom could be important factors controlling the seagrass ecosystem and other marine habitats in AKBL and other coastal lagoons in this region (Ayuttaka *et al*., 1994; Satumanatpan *et al*., 2011; Walter *et al*., 2018).

Currents and circulation patterns

In this paper, "current" refers to water movement and "circulation" refers to current pattern, represented by the distribution of current averaged over a defined period of time. Currents inside the lagoon are mainly controlled by tide. Tidal currents are strong during the rise and fall of water level (see Figure 7). The current speeds decrease to the lowest values at high and low tide. The maximum current speeds reach 0.4-0.5 $m \cdot s^{-1}$ at the lagoon mouth during spring tide. The maximum current speeds are less during the neap tide (approximately 0.1-0.2 $m \cdot s^{-1}$). These water currents remain consistent every tidal cycle, whereas water circulation within the lagoon is altered significantly in different monsoon periods (Figure 8). During the SW monsoon, water moves in a double-gyre circulation, forming a clockwise gyre at the northwestern part and counterclockwise gyre at the southeastern part of the lagoon. Near-surface and near-bottom currents flow toward the inner part of the lagoon in the same direction in shallow areas. However, at the central part of the lagoon, water flows toward the mouth. Here, the near-surface current flows much more weakly compared to the lower layers. During Transition 2 and the NE monsoon, double-gyre circulation also can be seen; however, the flows are in opposite directions from those described for the SW monsoon. During Transition 1, the model simulates a counterclockwise single-gyre circulation. Water circulation within the lagoon is generally sluggish, except during the SW monsoon.

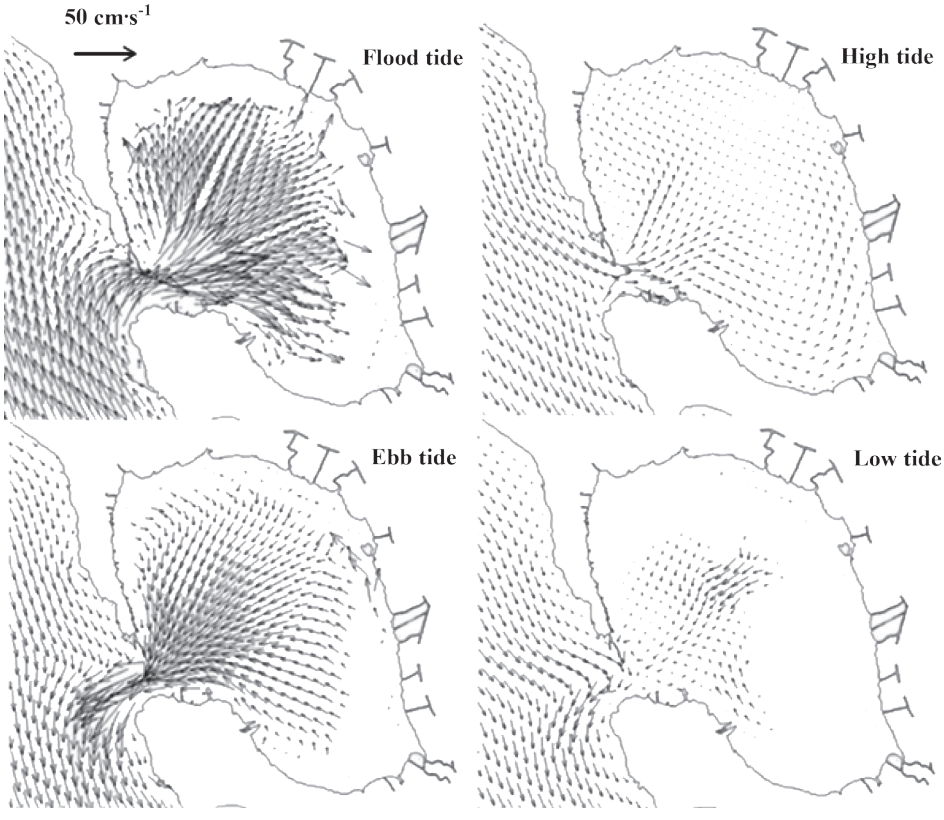

Figure 7. Simulated tidal current patterns and different tidal phases during spring tide.

Water temperature and salinity variations and their roles

Observed and simulated results correspondingly showed that there is significant variation in water temperature and salinity within the lagoon (Figure 9). Water temperature was highest (>32 ºC) in April to May, during Transition 1. It decreased during the SW monsoon and was lowest in the NE monsoon (<29 ºC). Moderate water temperature was observed during Transition 2. There were no significant differences between the water temperature within the lagoon and the outer sea. Salinity was highest (>31 psu) during Transition 1. It decreased rapidly to the lowest levels (<29 psu) during the SW monsoon, and then gradually increased. The salinity within the lagoon became significantly lower than the outer sea during the SW monsoon and Transition 2. This spatial variation in water temperature and salinity could result in differences in water density between lagoon and the outer sea. Influences of these differences are discussed below.

To evaluate influences of variation in water temperature and salinity on water circulation within the lagoon, hydrodynamic simulations were run both with and without water density variations (with density and without density). The simulations without density applied constant water temperature (28 °C) and salinity (31 psu), while the simulations with density applied varying water density values calculated from simulated water temperature and salinity. Figures 10, 11 and 12 show average flow velocity across the A-A axis and at the lagoon's mouth, at the near-surface and near-bottom layers, respectively. Results demonstrate that there were no significant differences between circulation patterns of the simulations with and without density. This indicates that water circulation within the lagoon is largely controlled by topography, tide and monsoonal winds. It is worth noting that there are significant differences in circulation patterns between the simulations with and without density for the outer sea during the SW monsoon and Transition 2. Less significant differences can be seen during the NE monsoon and Transition 1. This might be attributable to increased freshwater influxes to this area causing reduced salinity of thenear-surface water compared to the near-bottom water. Mechanisms governing this phenomenon require further investigation and are beyond the scope of this study.

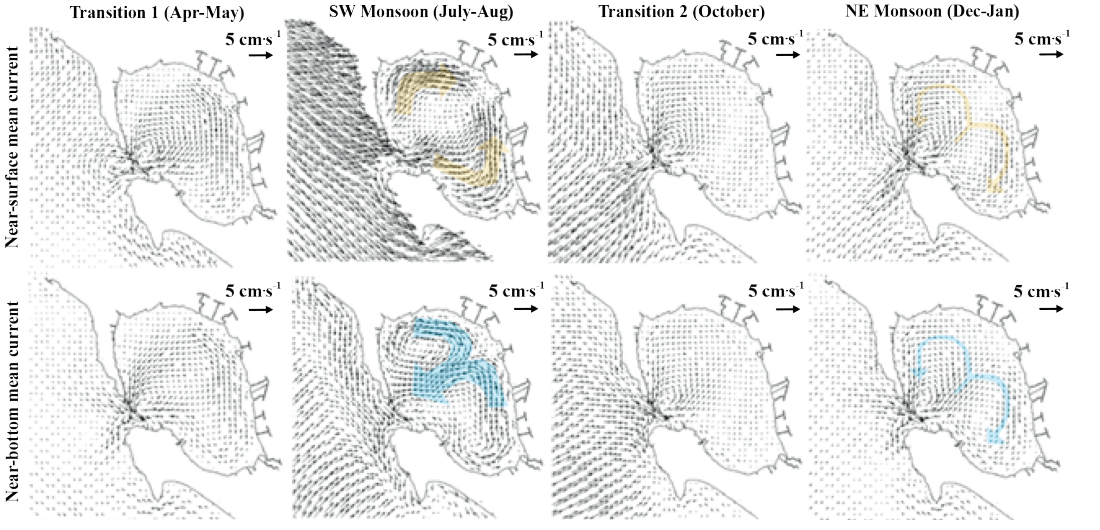

Figure 8. Simulated monthly mean flow velocity at near-surface (upper row) and at near-bottom (lower row) of AKBL and the outer sea during different monsoon periods.

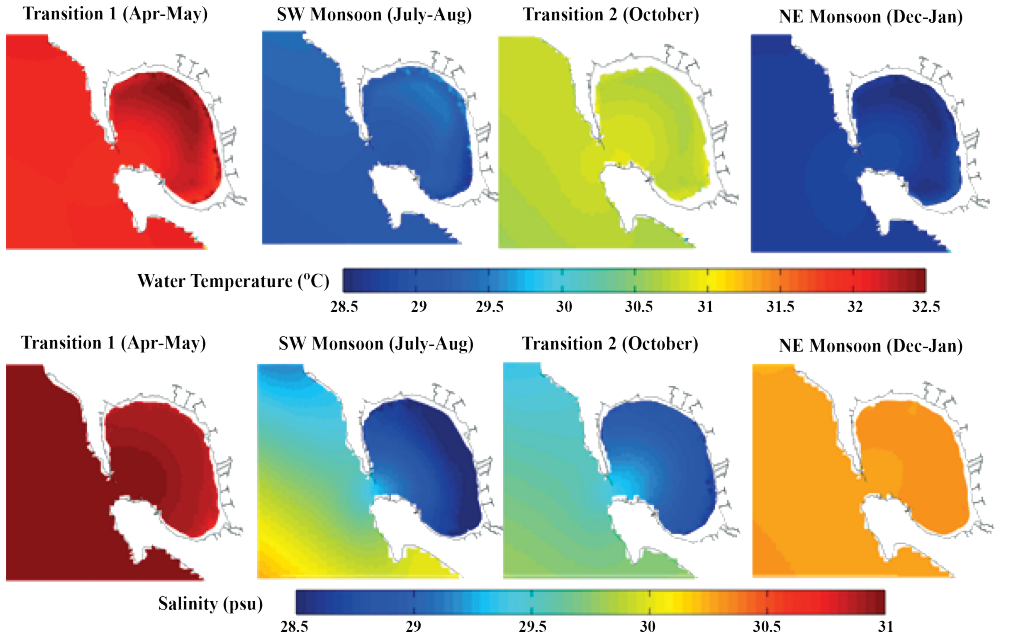

Figure 9. Simulated average near-surface water temperature (upper row) and salinity (lower row) of AKBL over different monsoon periods.

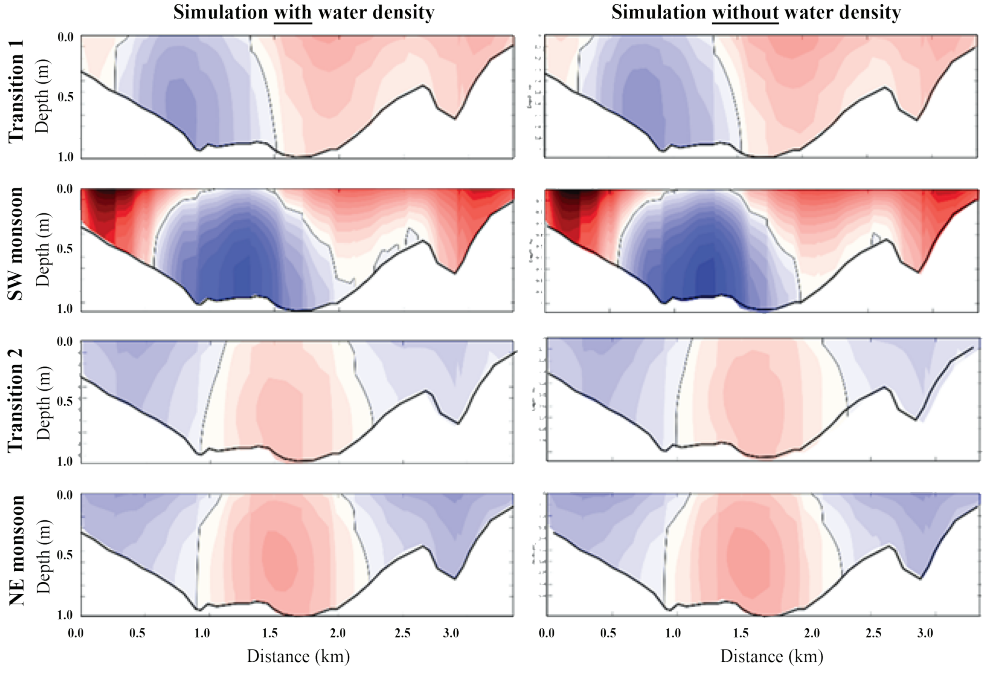

Figure 10. Mean flow velocity across the lagoon width (Section A-A) from simulations with and without variation in water density.

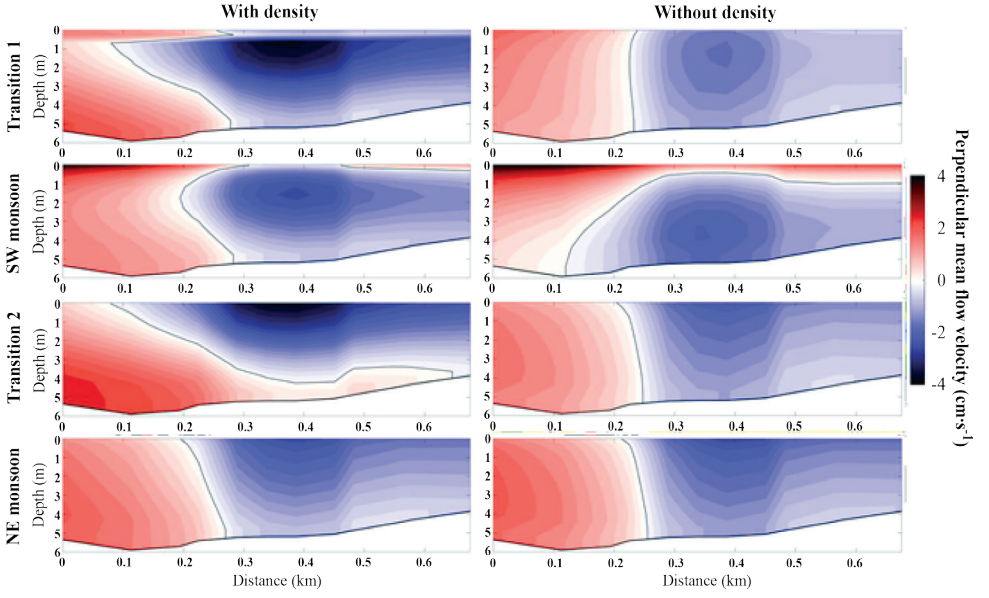

Figure 11. Mean flow velocity across the lagoon's mouth from simulations with and without variation in water density.

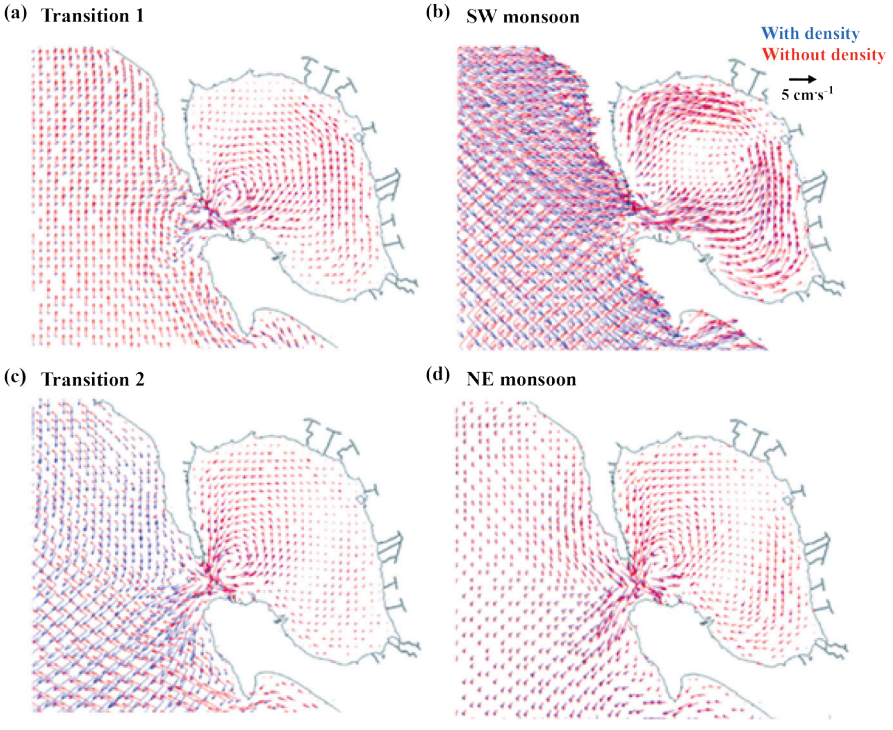

Figure 12. Comparisons of monthly-averaged near-surface flow velocity fields during (a) Transition 1, (b) SW monsoon, (c) Transition 2, and (d) NE monsoon from simulations with and without variation in water density.

Interactions between tropical coastal lagoons and their outer seas

We investigated the interactions using levels of exchange between the lagoon and the outer sea. The water exchanges were represented by flushing times of the water body (Monsen *et al*., 2002; Pokavanich and Alosairi, 2014). Higher exchange can result in shorter flushing time and vice versa. In this study, the seasonal flushing times were examined using conservative tracer simulation. The flushing times were determined when average tracer concentration within the lagoon had decreased to 10 % of the original released concentration. In other words, the flushing time is the time required for the 90 % of the lagoon water to be replaced by the outer sea water. Similar analysis was carried out by Pokavanich and Alosairi (2014).

Results suggested that flushing times of AKBL are short, ranging between 3 and 10 days (Figure 13). The times also vary significantly in different monsoon periods. The flushing time is shortest during the SW monsoon and is longest during Transition 1. The flushing times are similar in Transition 2 and the NE monsoon. The variation in flushing times is associated with seasonal water circulations within the lagoon. The flushing in Transition 1 is slowed by the sluggish single-gyre circulation that forces water to travel the greatest distance within the lagoon. The double-gyre circulation requires about half of the travel distance. The double-gyre circulation with stronger currents brings forth the shortest flushing time during the SW monsoon.

Results of flushing time analysis for the SW monsoon and Transition 2, shown in Figure 13b and Figure 13c, indicate notable differences between the simulations run with and without density. The flushing times of the simulations without density are longer than the simulations with density by about

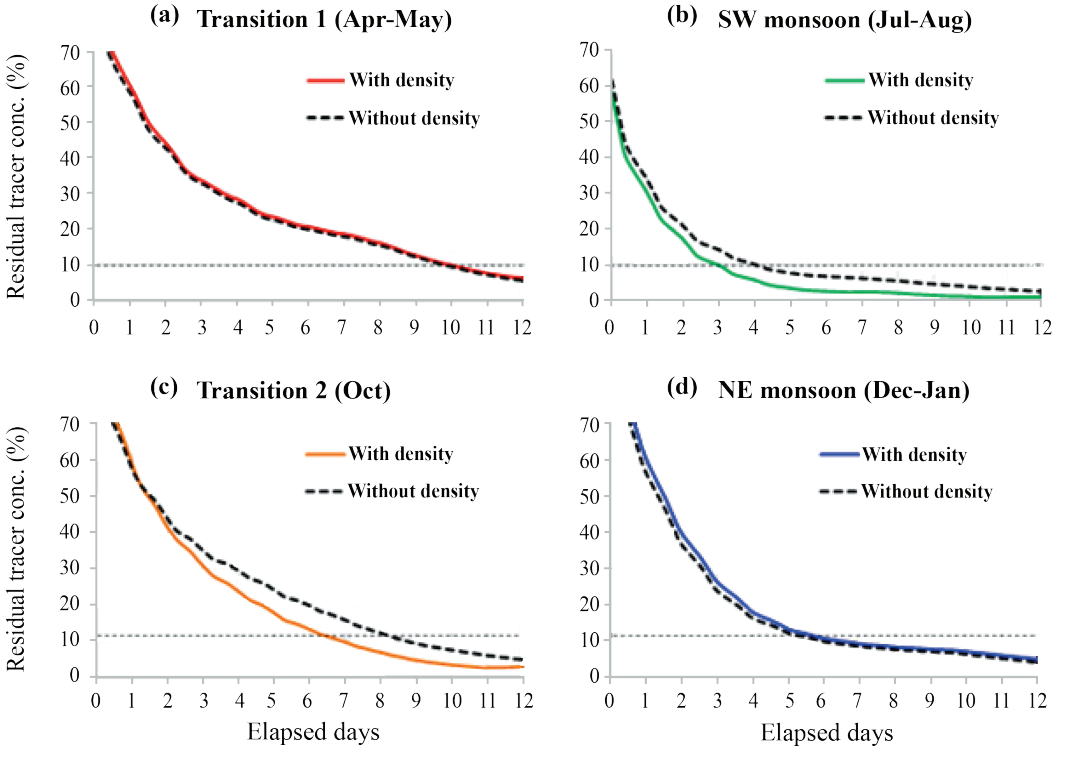

Figure 13. Tidally averaged concentration of tracer inside the lagoon during (a) Transition 1, (b) SW monsoon, (c) Transition 2 and (d) NE monsoon from simulations with and without variation in water density.

one day. This was not the case for Transition 1 or the NE monsoon. These differences in simulation results can be associated with seasonal water density differences between the lagoon and the outer sea governed by seasonal variations of the water temperature and the salinity. Simulated average water densities of water in the lagoon and in the outer sea are 1,017.93 and 1,018.06 $kg \cdot m^{-3}$, respectively, during Transition 1; 1,017.32 and 1,018.08 $kg \cdot m^{-3}$ during the SW monsoon; 1,017.01 and 1,017.43 $kg \cdot m^{-3}$ during Transition 2; and 1,018.63 and 1,018.60 $kg \cdot m^{-3}$ during the NE monsoon. The density differences between the lagoon and the outer sea are highest during the SW monsoon (-0.76 $kg \cdot m^{-3}$) and Transition 2 (-0.42 $kg \cdot m^{-3}$), and lower during Transition 1 (-0.14 $kg \cdot m^{-3}$) and the NE monsoon (+0.03 $kg \cdot m^{-3}$). Therefore, besides the water circulation within AKBL, density differences can result in varying rates of water exchange between the lagoon and the outer sea. The density differences induce thermohaline currents at the mouth that can enhance or diminish water exchange.

CONCLUSION

This study applied data from computer simulations validated with field measurements to investigate seasonal characteristics of currents, circulations, and interactions between AKBL and the outer sea. The results suggest that AKBL can serve as an example for other shallow tropical coastal lagoons, which are numerous and widely distributed around the world. It also demonstrated that currents within the lagoon are controlled by topography and tides. Tidal currents are strong and create conditions that favor mixing, resulting in homogeneous water properties horizontally and vertically within the lagoon. Monsoonal winds play an important role in controlling water circulation within the lagoon. Strongest circulation and the shortest flushing time were observed during the SW monsoon (July-September), while the weakest circulation and the longest flushing time occurred during Transition 1 (April-May). The results reveal that the degree of interaction between tropical coastal lagoons and their outer sea can vary significantly by season and is associated with the thermohaline circulation at the mouth.

It can be concluded that a two-dimensional hydrodynamic simulation forced by accurate topography, prevailing wind and tide can reasonably model seasonal water circulation patterns of tropical coastal lagoons. However, a three-dimensional model of the lagoon and the outer sea with realistic thermohaline effects is needed to accurately model the interactions between tropical coastal lagoons and their outer seas.

ACKNOWLEDGEMENTS

This work was supported by the Faculty of Fisheries, Kasetsart University. Special thanks are given to the KKBRD center for providing support during field observations. Lastly, the authors express their gratitude to the late Assoc. Prof. Chittima Aryuthaka, deceased on 1st December 2017, who provided encouragement for us to pursue this study.

LITERATURE CITED

Ayuttaka, J., S. Sungthong and K. Awaivanonth. 1994. **Seagrass beds in Kung Krabaen Bay, Chantaburi Province.** In: Department of Fisheries Seminar Report, 16-18 September 1993. Department of Fisheries, Bangkok, Thailand.

Barnes, R.S.K. 1980. **Coastal Lagoons.** Cambridge University Press, Cambridge, UK. 106 pp.

Deltares. 2018a. **Delft3D-FLOW, Simulation of Multi-Dimensional Hydrodynamic Flows and Transport Phenomena, Including Sediments, User Manual, Version 3.15.** MH Delft, Netherlands. 672 pp.

Deltares. 2018b. **D-Water Quality Processes Library Description, Detailed description of Processes, Technical Reference Manual, Version 5.01.** MH Delft, Netherlands. 460 pp.

Global Monitoring and Forecasting Center. 2016. **Global ocean 1/12° physics analysis and forecast updated daily.** https://resources.marine.copernicus.eu/?option=com_csw&view=details&product_id=GLOBAL_REANALYSIS_PHY_001_030. Cited 5 Mar 2020.

Global Monitoring and Forecasting Center. 2018. **Glorys12v1-global ocean physical reanalysis product, e.u. copernicus marine service information.** https://resources.marine.copernicus.eu/?option=com_csw&view=details&product_id=GLOBAL_REANALYSIS_PHY_001_030. Cited 5 Mar 2020.

Guyondet, T. and V.G. Koutitonsky. 2008. Tidal and residual circulations in coupled restricted and leaky lagoons. **Estuarine, Coastal and Shelf Science** 77(3): 396-408.

Harrigan, S., E. Zsoter, C. Barnard, F. Wetterhall, P. Salamon and C. Prudhomme. 2019. **River discharge and related historical data from the Global Flood Awareness System.** https://cds.climate.copernicus.eu/cdsapp#!/dataset/cems-glofas-historical?tab=form. Cited 10 Jun 2021.

Hersbach, H., B. Bell, P. Berrisford *et al*. 2020. The ERA5 global reanalysis. **Quarterly Journal of the Royal Meteorological Society** 146: 1999-2049.

Hersbach, H., B. Bell, P. Berrisford, G. Biavati, A. Horányi, J. Muñoz-Sabater, J. Nicolas, C. Peubey, R. Radu, I. Rozum, D. Schepers, A. Simmons, C. Soci, D. Dee and J.N. Thépaut. 2018a. **ERA5 hourly data on pressure levels from 1979 to present.** https://cds.climate.copernicus.eu/cdsapp#!/dataset/reanalysis-era5-pressure-levels?tab=overview. Cited 3 Feb 2021.

Hersbach, H., B. Bell, P. Berrisford, G. Biavati, A. Horányi, J. Muñoz-Sabater, J. Nicolas, C. Peubey, R. Radu, I. Rozum, D. Schepers, A. Simmons, C. Soci, D. Dee and J.N. Thépaut. 2018b. **ERA5 hourly data on single levels from 1979 to present.** https://cds.climate.copernicus.eu/cdsapp#!/dataset/reanalysis-era5-single-levels?tab=overview. Cited 3 Feb 2021.

Higuchi, M., M. Anongponyoskun, J. Phaksopa and H. Onishi. 2020. Influence of monsoon-forced Ekman transport on sea surface height in the Gulf of Thailand. **Agriculture and Natural Resources** 54: 205-210. DOI: 10.34044/j.anres.2020.54.2.12.

Kennish, M.J. and H.W. Paerl. 2010. **Coastal lagoons critical habitats of environmental change** In: Coastal Lagoons: Critical Habitats of Environmental Change (eds. M.J. Kennish and H.W. Paerl), pp. 1-16. CRC Press, Florida, USA.

Kjerve, B. 1986. **Comparative oceanography of coastal lagoons.** In: Estuarine Variability (ed. D.A. Wolfe), pp. 63-81. Academic Press, New York, USA.

Monsen, N.E., J.E. Cloern, L.V. Lucas and S.G. Monismith. 2002. A Comment on the use of flushing time, residence time, and age as transport time scales. **Limnology and Oceanography** 47(5): 1545-1553. DOI: 10.4319/lo.2002.47.5.1545.

Pokavanich, T. and Y. Alosairi. 2014. Summer flushing characteristics of Kuwait Bay. **Journal of Coastal Research** 30(5): 1066-1073. DOI/10.2112/JCOASTRES-D-13-00188.1.

Pokavanich, T., A. Buranapratheprat and C. Aryuthaka. 2018. **Hydrodynamics modelling of Kung Krabaen Lagoon, Chanthaburi, Thailand.** Proceeding of the SIBE2017-MATEC Web of Conferences conference 2018: 1-6. DOI: 10.1051/matecconf/201814705009.

Sangrungruang, C., W. Sakares, M. Anongponyoskun and B. Damrak. 1999. **The environment impact of shrimp culture on physical characteristics, soil qualities and seawater qualities of Kung Krabaen Bay before seawater irrigation construction.** In: 10th Year of Technical Work: Kung Krabean Bay Royal Development Study Center (ed. Kung Krabaen Bay Fisheries Development Study Center), pp. 47-117. Kung Krabaen Bay Fisheries Development Study Center, Chanthaburi, Thailand.

Sasaki, T. and H. Inoue. 1985. **Studies on fundamental environments in the Kung Kraben Bay, Eastern Thailand: Hydraulic environments.** In: Mangrove Estuarine Ecology in Thailand, Thai-Japanese Cooperative Research Project on Mangrove Productivity and Development, 1983-1984 (ed. K. Nozawa), pp. 77-98. Ministry of Education, Science and Culture, Tokyo, Japan.

Satumanatpan, S., S. Thummikkapong amd K. Kanongdate. 2011. Biodiversity of benthic fauna in the seagrass ecosystem of Kung Krabaen Bay, Chantaburi Province, Thailand. **Songklanakarin Journal of Science and Technology** 33: 341-348.

Sriyanie, M. 2013. **Lagoons and Estuaries: Coastal Ecosystems Series,** Vol. 4. International Union for Conservation of Nature, Colombo, Sri Lanka. 84 pp.

Sylaios, G.K., V.A. Tsihrintzis, A. Christos, A.C. Tsikliras and K. Haralambidou. 2005. Exchange dynamics through the mouth of a coastal lagoon. **Journal of Marine Environmental Engineering** 8: 1-19.

Walter, R.K., E.J. Rainville and J.K. O'Leary. 2018. Hydrodynamics in a shallow seasonally low-inflow estuary following eelgrass collapse. **Estuarine, Coastal and Shelf Science** 213: 160-175. DOI: 10.1016/j.ecss. 2018.08.026.